The Journal of Chemical Physics

Nonequilibrium free-energy profile of charge-transfer reaction in polarizable solvent studied using solvent-polarizable three-dimensional reference interaction-site model theory

Cite as: J. Chem. Phys. **153**, 034502 (2020); https://doi.org/10.1063/5.0013083
Submitted: 08 May 2020 . Accepted: 01 July 2020 . Published Online: 20 July 2020

Tsuyoshi Yamaguchi, and Norio Yoshida

The Journal of Chemical Physics ARTICLE scitation.org/journal/jcp

Nonequilibrium free-energy profile of charge-transfer reaction in polarizable solvent studied using solvent-polarizable three-dimensional reference interaction-site model theory

Cite as: J. Chem. Phys. 153, 034502 (2020); doi: 10.1063/5.0013083
Submitted: 8 May 2020 • Accepted: 1 July 2020 •
Published Online: 20 July 2020

Tsuyoshi Yamaguchi[1,a)] and Norio Yoshida[2,a)]

AFFILIATIONS

[1]Graduate School of Engineering, Nagoya University, Chikusa, Nagoya 464-8603, Japan
[2]Department of Chemistry, Graduate School of Science, Kyushu University, 744 Motooka, Nishiku, Fukuoka 819-0395, Japan

[a)]**Authors to whom correspondence should be addressed:** yamaguchi.tsuyoshi@material.nagoya-u.ac.jp and noriwo@chem.kyushu-univ.jp

ABSTRACT

The effects of the electronic polarization of solvent on the nonequilibrium free-energy profiles of charge-transfer reactions were studied using integral equation theory. Employing the solvent-polarizable three-dimensional reference interaction-site model theory, recently proposed by us, we first present a theoretical formalism that gives the free-energy profile in polarizable solvents. We then perform numerical calculations on three model systems. We demonstrate that electronic polarization of the solvent alters the solvent reorganization energy in two different ways. The first is the reorganization of the equilibrium solvation structure through the modification of the solute–solvent interaction, and the second is the stabilization of the nonequilibrium solvent fluctuation through the electronic polarization. The former increases, whereas the latter decreases the reorganization energy. In our model calculations, the solvent reorganization energy is reduced because the latter makes a larger contribution than does the former.

I. INTRODUCTION

Charge transfer is an elementary redox reaction process that plays important roles in various fields of chemistry, such as electrochemistry, biochemistry, and others.[1] A charge-transfer reaction in solution is coupled to the thermal fluctuation of the surrounding solvent; hence, an understanding of solvent effects is crucial.[2] A charge-transfer reaction is a nonadiabatic transition between two electronic states, where the transition occurs when the energies of the two states are almost identical. Since the charge transfer significantly alters the electrostatic interaction between solute and solvent, the energy difference between the reactant and product states fluctuates through the thermal fluctuation of solvent molecules. Therefore, a reaction coordinate of a charge-transfer reaction is the collective mode of the nuclear coordinates of solvent molecules, and the free-energy profile along the reaction coordinate, referred to as the "solvation coordinate," plays an essential role in the understanding of charge-transfer reactions in solution. According to the Marcus theory, in particular, there are two important parameters of free-energy profiles: the Gibbs energy of the reaction and the solvent reorganization energy.[2]

The most important mode of a solvent is the reorientation in polar solvents. A permanent dipole moment fixed to a solvent changes its orientation, together with the rotation of the solvent, and the fluctuation of the orientation of the permanent dipole is coupled to the charge-transfer reaction through the dipolar solvation of

the reactant and product states. In addition to a permanent dipole moment, a solvent molecule possesses an induced dipole moment due to the electronic polarization, and the induced dipole moment is also coupled to the charge-transfer reaction of a solute because the induced dipole varies in accordance with the nuclear motion of the solvent.[3–6]

The induced dipole moment is coupled to the charge-transfer reaction in a way different from that of the permanent dipole in terms of the time scale. Since the motion of an electron is much faster than that of a nucleus, the permanent dipole moment of the solvent is fixed upon the charge transfer of the solute. On the other hand, the induced dipole moment can immediately follow the charge transfer. The product state can thus be immediately stabilized by the induced dipole moment. Although the equilibrium solvation by the induced dipole moment is usually much weaker than that by the permanent dipole moment, the former may play an important role in the nonequilibrium free-energy profile of a charge-transfer reaction.

There are two computational methods for calculating the nonequilibrium free-energy profile of the charge-transfer reaction in solution from microscopic intermolecular interactions. The first is a molecular simulation method, such as molecular dynamics (MD) or Monte Carlo (MC) simulations.[7,8] With molecular simulation, one can obtain an exact free-energy profile within the limitations of the system size, statistical sampling, and molecular model. However, because the calculation of the free energy far from the equilibrium states of the reactant and product is required, the employment of some type of biased sampling is inevitable, the computational cost of which is much greater than that of the equilibrium runs of the reactant and product. Although the inclusion of the electronic polarization of the solvent is possible by using polarizable solvent models,[4–6,8] the computational cost of polarizable models is usually much larger than that of rigid charge models. Therefore, although molecular simulation has been applied to the nonequilibrium free-energy profiles of simple systems, its application to complicated systems such as proteins and interfaces is not so easy, particularly when the electronic polarization of the solvent is taken into account.

The second method is the use of integral equation theories based on statistical mechanics. Since integral equation theories treat correlation functions after statistical averaging, they are free from errors associated with finite system size and poor statistical sampling. In addition, computation using integral equation theories is usually much faster than that using molecular simulations. On the other hand, integral equation theories suffer from some systematic errors associated with approximations introduced through their derivation.

The reference interaction-site model (RISM) theory is a representative integral equation theory of liquids.[9] A polyatomic solvent molecule is approximated as a set of interaction sites in the RISM theory, and the correlation functions of the site density are calculated. With hypernetted chain (HNC) or Kovalenko–Hirata (KH) closures, the solvation free energy is also given in a closed form. The RISM theory has been successfully applied to the nonequilibrium free-energy profiles of simple charge-transfer reactions in nonpolarizable solvents.[10–13] The three-dimensional (3D) version of the RISM theory, referred to as the 3D-RISM theory, has also been employed to calculate the solvation free energy of proteins in water and the liquid structure of interfaces.[14–19]

Since the RISM theory treats the intermolecular interaction as the sum of isotropic site–site interaction potentials, it is impossible to include induced dipole moments directly. Instead, the charge response kernel (CRK) model, proposed by Morita and Kato, can introduce the intramolecular electronic polarization into the RISM theory. The CRK model describes the intramolecular electronic polarization as the linear response of the partial charge on a site to the electrostatic potentials on intramolecular sites.[20,21] Since the isotropic nature of the site–site potential is conserved in the CRK model, it can be combined with the RISM theory with relative ease. The combination of the CRK model and the conventional one-dimensional (1D) RISM theory was first proposed by Naka *et al.*,[22] and its 3D extension, the solvent-polarizable 3D RISM (sp-3D-RISM) theory, was reported by us very recently.[23]

In this work, the nonequilibrium free-energy profile of charge-transfer reactions in polarizable solvents is calculated based on our sp-3D-RISM theory. We first extend the theoretical scheme to calculate the free-energy profile in nonpolarizable solvents by the RISM theory to solvent-polarizable systems. Numerical calculations are then performed on some model systems, and the effects of the electronic polarization of the solvent on charge-transfer reactions are discussed.

II. THEORY

In this section, we present a theoretical formalism to calculate the nonequilibrium free-energy profile of a charge-transfer reaction in a polarizable solvent by means of the sp-3D-RISM theory. First, the thermodynamic argument employed in the conventional RISM theory for nonpolarizable solvents is reviewed in Sec. II A.[10,11] In Sec. II B, it is reformulated by statistical mechanics. In Sec. II C, the thermodynamic argument presented in Sec. II A is extended to polarizable solvents. In Sec. II D, validation is given from the viewpoint of statistical mechanics. Finally, in Sec. II E, the sp-3D-RISM theory is summarized.

A. Thermodynamic consideration: Nonpolarizable case

In nonpolarizable solvents, the classical Hamiltonians of the reactant and product states, denoted as $H_{\mathrm{R}}(\Gamma)$ and $H_{\mathrm{P}}(\Gamma)$, respectively, are defined as the functions of the nuclear coordinates of solvent molecules, Γ. Although intramolecular vibrational modes of the solute may also be coupled to the charge-transfer reaction, for simplicity, this is disregarded in this work. The solvation coordinate is usually defined as follows in terms of the energy difference of the two states:

$$\Delta H(\Gamma) \equiv H_{\mathrm{P}}(\Gamma) - H_{\mathrm{R}}(\Gamma). \tag{1}$$

What we are going to obtain are the free-energy profiles of both states, $F_{\mathrm{R}}(\Delta E)$ and $F_{\mathrm{P}}(\Delta E)$, as a function of $\Delta E = \Delta H(\Gamma)$.

Here, we introduce the intermediate state characterized by the Hamiltonian,

$$H_z(\Gamma) = (1-z)H_{\mathrm{R}}(\Gamma) + zH_{\mathrm{P}}(\Gamma), \tag{2}$$

where z is a real number. In particular, $z = 0$ and $z = 1$ stand for the reactant and product states, respectively. An important strategy is to identify the nonequilibrium state characterized by the solvation coordinate, $\Delta E = \Delta H(\Gamma)$, with the equilibrium state of an intermediate z-state whose equilibrium value of the solvation coordinate, $\Delta E^*(z)$, is equal to ΔE.[24]

The free-energy difference, $\Delta F_R(z) \equiv F_R(\Delta E^*(z)) - F_R(\Delta E^*(0))$, is equal to the work required to reorganize the solvent from the equilibrium state of the reactant to that of the z-state while keeping the solute in the reactant state. Such a change in the solvation state can then be established through the following pathway[10] [also presented schematically in Fig. 1(a)]:

(i) Remove a solute in the reactant state from the solution into vacuum. The work required in this process is given by $\Delta\mu_R$, where $\Delta\mu_R \equiv \Delta\mu(z = 0)$ denotes the solvation free energy of the reactant and $\Delta\mu(z)$ denotes that of the z-state.
(ii) Change the state of the solute from the reactant to the z-state. The work associated with this process is equal to $z\Delta E_{vac}$, where ΔE_{vac} denotes the energy difference between the product and reactant states in vacuum.
(iii) Solvate the z-state solute into the solution; the work of this process is given by $\Delta\mu(z)$.
(iv) Change the state of the solute from the z-state to the reactant while freezing the nuclear coordinates of the solvent; the work is equal to the energy difference, $\langle H_R(\Gamma) - H_z(\Gamma)\rangle_z = -z\Delta E^*(z)$, where the angular bracket with the suffix z denotes the equilibrium average of the z-state.

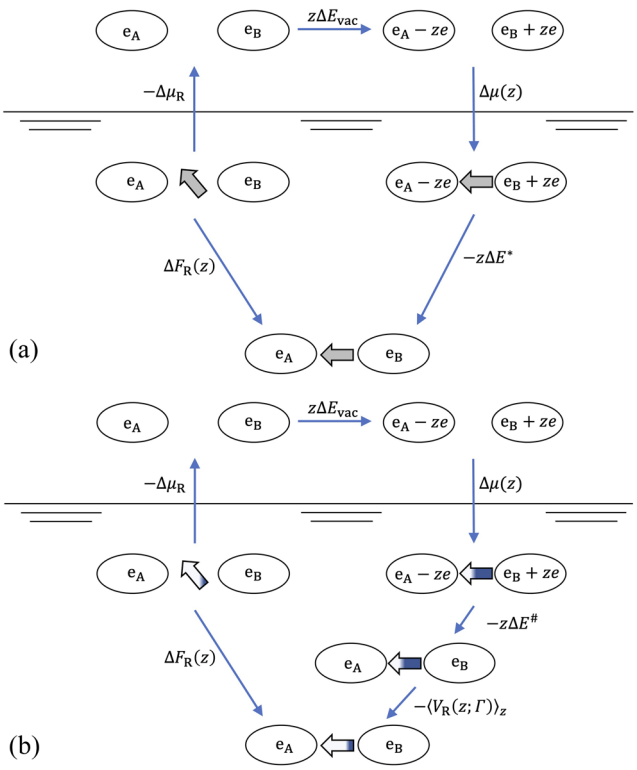

FIG. 1. Schematic of the thermodynamic pathways to calculate $\Delta F_R(z)$ (a) in a nonpolarizable solvent and (b) in a polarizable solvent. The colored gradation within the bold arrows in (b) represents the degree of electronic polarization.

These works are summarized as follows to give the required free-energy difference:

$$F_R(\Delta E^*(z)) - F_R(\Delta E^*(0)) = \Delta\mu(z) - \Delta\mu_R - z[\Delta E^*(z) - \Delta E_{vac}]. \tag{3}$$

The free-energy profile of the product state can also be evaluated as follows in a similar way:

$$F_P(\Delta E^*(z)) - F_P(\Delta E^*(1)) = \Delta\mu(z) - \Delta\mu_P + (1 - z)[\Delta E^*(z) - \Delta E_{vac}]. \tag{4}$$

The origin of the free energy is not specified in Eqs. (3) and (4) because only the differences from the values in their respective equilibrium solvation states are given.

B. Statistical mechanical derivation: Nonpolarizable case

The free-energy profile of the reactant state is defined by

$$\exp[-\beta F_R(\Delta E)] \equiv \frac{1}{\Xi}\int d\Gamma\delta[\Delta H(\Gamma) - \Delta E]\exp[-\beta H_R(\Gamma)], \tag{5}$$

where Ξ is the normalization factor, $\beta = 1/k_B T$, where k_B is the Boltzmann constant and T is the absolute temperature. Equation (5) is then transformed as follows:

$$F_R(\Delta E) = F_z(\Delta E) - z\Delta E, \tag{6}$$

where $F_z(\Delta E)$ denotes the free-energy profile of the z-state. Assuming that $F_z(\Delta E)$ is parabolic around its minimum, $\Delta E^*(z)$, then the chemical potential of the z-state, $\mu(z)$, is related to $F_z(\Delta E)$ as follows:

$$\mu(z) - \mu(0) = z\Delta E_{vac} + \Delta\mu(z) - \Delta\mu_R = F_z(\Delta E^*(z)) - F_R(\Delta E^*(0)) + \frac{1}{\beta}\ln\left[\frac{F_z''(\Delta E^*(z))}{F_R''(\Delta E^*(0))}\right], \tag{7}$$

where the chemical potential is described as the difference from the equilibrium state to eliminate the normalization factors associated with the integral over Γ and the measure associated with ΔE. From Eqs. (6) and (7), $F_z(\Delta E)$ is eliminated as follows:

$$F_R(\Delta E^*(z)) - F_R(\Delta E^*(0)) = \Delta\mu(z) - \Delta\mu_R - z[\Delta E^*(z) - \Delta E_{vac}] - \frac{1}{\beta}\ln\left[\frac{F_R''(\Delta E^*(z))}{F_R''(\Delta E^*(0))}\right]. \tag{8}$$

Here, $F_z''(\Delta E^*(z))$ is replaced with $F_R''(\Delta E^*(z))$ from the second derivative of Eq. (6).

Since $F_z(\Delta E)$ shows a minimum at $\Delta E^*(z)$, the derivative of Eq. (6) gives

$$F_z'(\Delta E^*(z)) = F_R'(\Delta E^*(z)) + z = 0, \tag{9}$$

which is further differentiated with respect to z as

$$F_R''\left(\Delta E^*(z)\right) = -\frac{dz}{d\Delta E^*(z)}. \tag{10}$$

The variable of the free-energy profile, $F_R(\Delta E)$, is then changed from ΔE to z through $\Delta E = \Delta E^*(z)$. The resultant free-energy profile, denoted as $\tilde{F}_R(z)$, is given by

$$\begin{aligned}\tilde{F}_R(z) &= F_R\left(\Delta E^*(z)\right) + \frac{1}{\beta}\ln\left[\left|\frac{dz}{d\Delta E^*(z)}\right|\right] \\ &= F_R\left(\Delta E^*(z)\right) + \frac{1}{\beta}\ln\left[F_R''\left(\Delta E^*(z)\right)\right].\end{aligned} \tag{11}$$

The second term represents the entropy associated with the measure for which Eq. (10) is substituted. The combination of Eqs. (8) and (11) yields

$$\tilde{F}_R(z) - \tilde{F}_R(0) = \Delta\mu(z) - \Delta\mu_R - z\left[\Delta E^*(z) - \Delta E_{vac}\right], \tag{12}$$

which is equivalent to Eq. (3).

C. Thermodynamic argument: Polarizable case

In this subsection, the conventional thermodynamic argument on nonpolarizable solvents is extended to solvents with electronic polarization. Polarizable solvent molecules possess intramolecular degrees of freedom associated with the electronic polarization, denoted as Q, in a collective way, in addition to the nuclear coordinate, Γ. The Hamiltonians of the reactant and product are the functions of both Q and Γ, denoted as $H_R(\Gamma, Q)$ and $H_P(\Gamma, Q)$, respectively. The intermediate z-state is then characterized by the Hamiltonian,

$$H_z(\Gamma, Q) = (1-z)H_R(\Gamma, Q) + zH_P(\Gamma, Q). \tag{13}$$

The solute–solvent interaction is assumed to be linear to the electronic polarization, and the electronic polarizability of the solvent is truncated at the linear order.

Since the time scale of the electron degrees of freedom is much faster than that of the nucleus, Q is considered to follow the value that minimizes the given Hamiltonian with the given Γ. The polarization that minimizes $H_z(\Gamma, Q)$ is a function of Γ, denoted as $Q_z(\Gamma)$. In particular, $Q_R(\Gamma)$ and $Q_P(\Gamma)$ are equivalent to $Q_0(\Gamma)$ and $Q_1(\Gamma)$, respectively.

In the z-state with a given nuclear configuration, Γ, the energy required to distort the electronic polarization from the stable state, $Q_z(\Gamma)$, to unstable one, $Q_R(\Gamma)$, is defined by

$$V_R(z;\Gamma) \equiv H_z(\Gamma, Q_R(\Gamma)) - H_z(\Gamma, Q_z(\Gamma)). \tag{14}$$

Due to the linear assumption of the electronic polarization, it is equal to the energy of polarization distortion from $Q_R(\Gamma)$ to $Q_z(\Gamma)$ in the reactant state as

$$V_R(z;\Gamma) = H_R(\Gamma, Q_z(\Gamma)) - H_R(\Gamma, Q_R(\Gamma)). \tag{15}$$

A similar definition is also applied to the product state as

$$\begin{aligned}V_P(z;\Gamma) &\equiv H_z(\Gamma, Q_P(\Gamma)) - H_z(\Gamma, Q_z(\Gamma)) \\ &= H_P(\Gamma, Q_z(\Gamma)) - H_P(\Gamma, Q_P(\Gamma)).\end{aligned} \tag{16}$$

The Proof of Eqs. (15) and (16) is described in detail in Sec. S-I of the supplementary material.

The transition energy from the reactant to the product is given as a function of Γ as follows:

$$\Delta H(\Gamma) \equiv H_P(\Gamma, Q_P(\Gamma)) - H_R(\Gamma, Q_R(\Gamma)). \tag{17}$$

An important point here is that the nuclear coordinate Γ is frozen, whereas the electronic polarization can follow the charge transfer. What we wish to obtain here are the free-energy profiles of the reactant and product, denoted as $F_R(\Delta E)$ and $F_P(\Delta E)$, respectively, as a function of $\Delta E = \Delta H(\Gamma)$.

The statistical average of $\Delta H(\Gamma)$ in the intermediate z-state is described as

$$\Delta E^*(z) \equiv \langle \Delta H(\Gamma)\rangle_z = \langle H_P(\Gamma, Q_P(\Gamma)) - H_R(\Gamma, Q_R(\Gamma))\rangle_z. \tag{18}$$

The contribution of the change in the electronic polarization is excluded from $\Delta E^*(z)$, to define $\Delta E^\#(z)$, as follows:

$$\begin{aligned}\Delta E^\#(z) &\equiv \langle H_P(\Gamma, Q_z(\Gamma)) - H_R(\Gamma, Q_z(\Gamma))\rangle_z \\ &= \Delta E^*(z) + \langle V_P(z;\Gamma)\rangle_z - \langle V_R(z;\Gamma)\rangle_z.\end{aligned} \tag{19}$$

In the thermodynamic argument in this subsection, the nonequilibrium ensemble of Γ corresponding to the solvation coordinate ΔE is identified with the equilibrium ensemble of the z-state at which $\Delta E^*(z) = \Delta E$. The transition from the reactant to the z-state can then be established through the following pathway [also presented schematically in Fig. 1(b)]. The processes (i)–(iii) below and the works they require are the same as those in the nonpolarizable case in Sec. II A.

(i) Remove a solute in the reactant state from the solution into vacuum; the work required in this process is given by $-\Delta\mu_R = \Delta\mu(z=0)$.
(ii) Change the state of the solute from the reactant to the z-state; the work associated with this process is equal to $z\Delta E_{vac}$.
(iii) Solvate the z-state solute into the solution; the work of this process is given by $\Delta\mu(z)$.
(iv) Change the state of the solute from the z-state to the reactant while freezing both the nuclear and electron coordinates of the solvent; the work is equal to $-z\Delta E^\#(z)$, where $\Delta E^\#(z)$ is defined by Eq. (19).
(v) The electronic polarization is altered from $Q_z(\Gamma)$ to $Q_R(\Gamma)$; the required energy is given by $-V_R(z;\Gamma)_z$, where $V_R(z;\Gamma)$ is defined by Eq. (14).

Summarization of the works required by the above processes yields the following:

$$\begin{aligned}F_R\left(\Delta E^*(z)\right) - F_R\left(\Delta E^*(0)\right) = \Delta\mu(z) - \Delta\mu_R - z\left[\Delta E^\#(z) - \Delta E_{vac}\right] \\ - \langle V_R(z;\Gamma)\rangle_z.\end{aligned} \tag{20}$$

The free-energy profile of the product is derived in a similar way as follows:

$$\begin{aligned}F_P\left(\Delta E^*(z)\right) - F_P\left(\Delta E^*(1)\right) = \Delta\mu(z) - \Delta\mu_P + (1-z) \\ \times \left[\Delta E^\#(z) - \Delta E_{vac}\right] - \langle V_P(z;\Gamma)\rangle_z.\end{aligned} \tag{21}$$

D. Statistical mechanical derivation: Polarizable case

The free-energy profile of the reactant state is defined in a similar way to Eq. (5) as follows:

$$\exp[-\beta F_{\mathrm{R}}(\Delta E)] \equiv \frac{1}{\Xi}\int d\Gamma \delta[\Delta H(\Gamma)-\Delta E]\exp[-\beta H_{\mathrm{R}}(\Gamma, Q_{\mathrm{R}}(\Gamma))], \tag{22}$$

which is transformed as

$$F_{\mathrm{R}}(\Delta E) = F_{\mathrm{z}}(\Delta E) - z\Delta E - \bar{V}(z;\Delta E). \tag{23}$$

Here, $\bar{V}(z;\Delta E)$ is defined as

$$\exp\left[\beta \bar{V}(z;\Delta E)\right] \equiv \frac{\int d\Gamma \delta[\Delta H(\Gamma)-\Delta E]\exp[\beta[(1-z)V_{\mathrm{R}}(z;\Gamma)+zV_{\mathrm{P}}(z;\Gamma)]\exp[-\beta H_z(\Gamma,Q_z(\Gamma))]]}{\int d\Gamma \delta[\Delta H(\Gamma)-\Delta E]\exp[-\beta H_z(\Gamma,Q_z(\Gamma))]}. \tag{24}$$

The relationship between the solvation free energy of the z-state and $F_{\mathrm{z}}(\Delta E)$ is given by Eq. (7) in the presence of the electronic polarization.

The free-energy profile is changed from the function of ΔE to that of z in the same way as Sec. II B to describe $\tilde{F}_{\mathrm{R}}(z)$ as Eq. (11). Then, Eqs. (7) and (23) are substituted into Eq. (11) to yield the following:

$$\tilde{F}_{\mathrm{R}}(z) - \tilde{F}_{\mathrm{R}}(0) = \Delta\mu(z) - \Delta\mu_{\mathrm{R}} - z\left[\Delta E^*(z) - \Delta E_{\mathrm{vac}}\right] - \bar{V}\left(z;\Delta E^*(z)\right) + \frac{1}{\beta}\ln\left[\frac{F_{\mathrm{R}}''\left(\Delta E^*(z)\right)}{F_{\mathrm{z}}''\left(\Delta E^*(z)\right)}\cdot\frac{F_{\mathrm{z}}''\left(\Delta E^*(0)\right)}{F_{\mathrm{R}}''\left(\Delta E^*(0)\right)}\right]. \tag{25}$$

According to Eq. (23), the second derivatives of $F_{\mathrm{R}}(\Delta E)$ and $F_{\mathrm{z}}(\Delta E)$ are related to each other as

$$F_{\mathrm{R}}''(\Delta E) = F_{\mathrm{z}}''(\Delta E) - \bar{V}''(z;\Delta E), \tag{26}$$

and the last term of the right-hand side of Eq. (25) does not disappear, contrary to that in the nonpolarizable case. However, since the absolute value of $\bar{V}(z;\Delta E)$ is small (as will be shown later in numerical calculations), we can introduce an approximation as $F_{\mathrm{R}}''(\Delta E) \simeq F_{\mathrm{z}}''(\Delta E)$ to neglect the last term.

We further introduce an approximation into Eq. (24), namely, that the fluctuations of $V_{\mathrm{R}}(z;\Gamma)$ and $V_{\mathrm{P}}(z;\Gamma)$ are small around the equilibrium z-state. In such a case, Eq. (24) is simplified as

$$\bar{V}\left(z;\Delta E^*(z)\right) \simeq (1-z)\langle V_{\mathrm{R}}(z;\Gamma)\rangle_{\mathrm{z}} + z\langle V_{\mathrm{P}}(z;\Gamma)\rangle_{\mathrm{z}}. \tag{27}$$

The substitutions of Eqs. (19) and (27) into Eq. (25) after neglecting the last term give

$$\tilde{F}_{\mathrm{R}}(z) - \tilde{F}_{\mathrm{R}}(0) = \Delta\mu(z) - \Delta\mu_{\mathrm{R}} - z\left[\Delta E^{\#}(z) - \Delta E_{\mathrm{vac}}\right] - \langle V_{\mathrm{R}}(z;\Gamma)\rangle_{\mathrm{z}}. \tag{28}$$

This equation, equivalent to Eq. (20), corresponds to Eq. (12) in the nonpolarizable case.

E. Brief overview of the sp-3D-RISM theory

In the RISM theory, a polyatomic molecule is regarded as a collection of interaction sites. The molecular geometry is characterized by the intramolecular correlation function, denoted as $\omega_{\nu\nu'}(r)$, where ν and ν' are indices of the interaction sites. The intermolecular interaction between interaction sites is usually approximated as the sum of the Lennard-Jones (LJ) and Coulomb potentials, and each interaction site is characterized by the LJ parameters and the partial charge, Q_ν. Although the partial charge is a constant in the conventional RISM theory for nonpolarizable molecules, the CRK model describes the intramolecular electronic polarization by extending Q_ν as the linear function of the electrostatic potentials on intramolecular interaction sites, $V_{\nu'}$, as follows:[20,21]

$$Q_\nu = Q_\nu^{\mathrm{vac}} + \sum_{\nu'} K_{\nu\nu'} V_{\nu'}, \tag{29}$$

where Q_ν^{vac} denotes the partial charge in vacuum and $K_{\nu\nu'}$ is referred to as the CRK.

The sp-3D-RISM theory is used to calculate the 3D solvation structure and the thermodynamic properties of a solute.[23] It requires the site–site partial structure factor of the solvent as an input. Since the partial charge on a solvent site in a neat solvent deviates from that in vacuum because of solvation, the partial charge in the neat solvent should also be calculated in advance. In the sp-3D-RISM theory, these properties of the neat solvent are obtained from the 1D-RISM based theory proposed by Naka *et al.*[22] In particular, the partial charge in the neat solvent, denoted as $Q_\nu^0 = Q_\nu^{vac} + \Delta Q_\nu^0$, is determined by

$$\Delta Q_\nu^0 = \sum_{\nu'} K_{\nu\nu'}\rho_{\nu'}\int_0^\infty \frac{Q_{\nu'}^0}{r} g_{\nu\nu'}(r) 4\pi r^2 dr, \tag{30}$$

where $\rho_{\nu'}$ and $g_{\nu\nu'}(r)$ denote the number density of the interaction site ν' and the site–site radial distribution function of the neat solvent, respectively. Equation (30) is coupled to the conventional 1D-RISM theory to determine both Q_ν^0 and $g_{\nu\nu'}(r)$ in a self-consistent way.

In the presence of a solute, the partial charge on a solvent site further deviates from Q_ν^0 because of the electrostatic potential induced by the solute. Since the electric potential of the solute is position-dependent, the partial charge also becomes heterogeneous as follows:

$$Q_\nu(\boldsymbol{r}) \equiv Q_\nu^0 + \delta\Delta Q_\nu(\boldsymbol{r}). \tag{31}$$

The polarization charge from the bulk solvent, denoted as $\delta\Delta Q_\nu(\boldsymbol{r})$, is given in the sp-3D-RISM theory by

$$\rho_\nu g_\nu(\boldsymbol{r})\delta\Delta Q_\nu(\boldsymbol{r}) = \sum_{\nu'} K_{\nu\nu'}\int \left\langle \rho_\nu(\boldsymbol{r})\rho_{\nu'}(\boldsymbol{r}')\right\rangle_{\mathrm{s}} V(\boldsymbol{r}')d\boldsymbol{r}', \tag{32}$$

where $g_\nu(\boldsymbol{r})$ denotes the distribution function of the solvent site ν and $\left\langle \rho_\nu(\boldsymbol{r})\rho_{\nu'}(\boldsymbol{r}')\right\rangle_{\mathrm{s}}$ is the intramolecular density–density correlation function. Calculation of the latter is described in detail in our previous paper.[23] In the polarization scheme IV of the sp-3D-RISM theory, the electrostatic potential, $V(\boldsymbol{r})$, is composed of three terms as follows:

$$V(\boldsymbol{r}) = V_{\mathrm{solu}}(\boldsymbol{r}) + V_{\mathrm{solv}}^{\mathrm{stat}}(\boldsymbol{r}) + V_{\mathrm{solv}}^{\mathrm{pol}}(\boldsymbol{r}). \tag{33}$$

The first term is the potential made by the solute charge, while the second and third are made by Q_ν^0 and $\delta\Delta Q_\nu(\boldsymbol{r})$ charges of the solvent, respectively. The latter two terms are described explicitly as

$$V^{\mathrm{stat}}_{\mathrm{solv}}(\boldsymbol{r}) = \sum_{\nu'} \int \rho_{\nu'} g_{\nu'}(\boldsymbol{r}') \frac{Q^0_{\nu'}}{|\boldsymbol{r}-\boldsymbol{r}'|} \mathrm{erf}\left(\alpha|\boldsymbol{r}-\boldsymbol{r}'|\right) d\boldsymbol{r}', \quad (34)$$

$$V^{\mathrm{pol}}_{\mathrm{solv}}(\boldsymbol{r}) = \sum_{\nu'} \int \rho_{\nu'} g_{\nu'}(\boldsymbol{r}') \frac{\delta\Delta Q_{\nu'}(\boldsymbol{r}')}{|\boldsymbol{r}-\boldsymbol{r}'|} \mathrm{erf}\left(\alpha|\boldsymbol{r}-\boldsymbol{r}'|\right) d\boldsymbol{r}', \quad (35)$$

where α is the parameter introduced to exclude the self-interaction effectively.

The interaction potential is renormalized because of the electronic polarization as

$$u^{\mathrm{CRK}}_{\nu}(\boldsymbol{r}) = u_{\nu}(\boldsymbol{r}) + \frac{1}{2}\delta\Delta Q_{\nu}(\boldsymbol{r})\left(V_{\mathrm{solu}}(\boldsymbol{r}) + V^{\mathrm{stat}}_{\mathrm{solv}}(\boldsymbol{r}) + V^{\mathrm{pol}}_{\mathrm{solv}}(\boldsymbol{r})\right) + Q^0_{\nu} V^{\mathrm{pol}}_{\mathrm{solv}}(\boldsymbol{r}), \quad (36)$$

where $u_{\nu}(\boldsymbol{r})$ denotes the bare interaction potential on the solvent site ν when its partial charge is equal to Q^0_{ν}. The solvation structure, $g_{\nu}(\boldsymbol{r})$, is obtained by solving the 3D-RISM equation with the renormalized potential, $u^{\mathrm{CRK}}_{\nu}(\boldsymbol{r})$. In the sp-3D-RISM theory, $g_{\nu}(\boldsymbol{r})$ and $\delta\Delta Q_{\nu}(\boldsymbol{r})$ are determined simultaneously in a self-consistent way.

With the HNC or the KH closures, the solvation free energy of the solute, $\Delta\mu$, is expressed in an analytical way as follows:

$$\Delta\mu = \Delta\mu_{\mathrm{sc}} - \sum_{\nu} \rho_{\nu} \int g_{\nu}(\boldsymbol{r})\left(Q^0_{\nu} + \frac{1}{2}\delta\Delta Q_{\nu}(\boldsymbol{r})\right) V^{\mathrm{pol}}_{\mathrm{solv}}(\boldsymbol{r}) d\boldsymbol{r}, \quad (37)$$

where $\Delta\mu_{\mathrm{sc}}$ is the Singer–Chandler formula of the solvation free energy.[9,25]

The energy required to distort the electronic polarization of the solvent, $\langle V_{\mathrm{R}}(z;\Gamma)\rangle_z$, is described as follows:

$$\langle V_{\mathrm{R}}(z;\Gamma)\rangle_z = -\frac{1}{2}\sum_{\nu} \rho_{\nu} \int g^z_{\nu}(\boldsymbol{r})\left(\delta\Delta Q^{\mathrm{R}}_{\nu}(\boldsymbol{r};z) - \delta\Delta Q^z_{\nu}(\boldsymbol{r};z)\right) \times \left(V^{\mathrm{R}}_{\mathrm{solu}}(\boldsymbol{r}) - V^z_{\mathrm{solu}}(\boldsymbol{r})\right) d\boldsymbol{r}, \quad (38)$$

where the superscripts R and z indicate the corresponding functions in the reactant or the z-state, respectively, and the calculation of the polarization charge, $\delta\Delta Q^{\mathrm{R}}_{\nu}(\boldsymbol{r};z)$, is performed by fixing the site distribution to $g^z_{\nu}(\boldsymbol{r})$ while applying $V^{\mathrm{R}}_{\mathrm{solu}}(\boldsymbol{r})$ to the electronic polarization. The expression for $\langle V_{\mathrm{P}}(z;\Gamma)\rangle_z$ is given by replacing the R with P.

With the use of the sp-3D-RISM theory for the nonequilibrium free-energy profile, the relaxation of the polarization charge density, $\delta\Delta Q^{\mathrm{R}}_{\nu}(\boldsymbol{r};z) - \delta\Delta Q^z_{\nu}(\boldsymbol{r};z)$, can be evaluated *after* the calculation of the ensemble-averaged solvation structure, $g^z_{\nu}(\boldsymbol{r})$. In molecular simulation, on the other hand, the relaxation of the electronic polarization should be calculated for each nuclear configuration of biased sampling *prior to* the ensemble average. Since the calculation of the relaxed electronic polarization is a time-consuming process in molecular simulation, our present method possesses large computational advantage over molecular simulation.

The transition energy under frozen polarization, $\Delta E^{\#}(z)$, is given by

$$\Delta E^{\#}(z) = \sum_{\nu} \rho_{\nu} \int g^z_{\nu}(\boldsymbol{r})\left(Q^0_{\nu} + \delta\Delta Q^z_{\nu}(\boldsymbol{r};z)\right)\left(V^{\mathrm{P}}_{\mathrm{solu}}(\boldsymbol{r}) - V^{\mathrm{R}}_{\mathrm{solu}}(\boldsymbol{r})\right) d\boldsymbol{r}, \quad (39)$$

and $\Delta E^{*}(z)$ can be calculated from $\langle V_{\mathrm{R}}(z;\Gamma)\rangle_z$, $\langle V_{\mathrm{P}}(z;\Gamma)\rangle_z$, and $\Delta E^{\#}(z)$ using Eq. (19).

III. COMPUTATIONAL DETAILS

In the present study, we examined three model systems: a sodium atom, whose charge changes from 0 to $+e$, the Fe(II)–Fe(III) interionic charge transfer, and the electronic transition of *p*-nitroaniline (pNA) in an aqueous solution. pNA is a planar, push–pull type aromatic dye whose dipole moment increases upon electronic transition from the ground state to the first excited state. In this work, the ground and excited states are regarded as the reactant and product states, respectively. In all cases, the solutes are infinitely dilute in the aqueous solution.

Prior to the calculations on solute–solvent systems, the solvent-polarizable RISM (sp-RISM) calculation for the neat solvent system was conducted. Details of the sp-RISM computational procedure for solvent systems are reported in our previous paper.[23] The temperature and the number density were set at 298.0 K and 0.033 34 Å^{-3}, respectively. The LJ parameters of water were taken from the simple point charge (SPC) model with modified hydrogen parameters, σ_{H} = 1.00 Å and ϵ_{H} = 0.046 kcal/mol. The CRK and molecular structure of solvent water were taken from the literature.[26,27] The dielectrically consistent RISM (DRISM) method was employed for the dielectric correction, where the dielectric constant of solvent water was set at 78.5.[28] The number of grid points for the computation of the neat solvent system was 16 384 with a grid width of 0.01 Å.

The LJ parameters for the Na atom, σ_{Na} = 4.07 Å and ϵ_{Na} = 0.0005 kcal/mol, were taken from those for the Na^+ ion proposed by Åqvist.[29] For solute Fe ions, we used σ_{Fe} = 3.92 Å and ϵ_{Fe} = 0.02 kcal/mol, taken from the MM3 force field parameter set.[30] The distance between the Fe(II) and Fe(III) ions was set to 5.0 Å because this was found to be favorable for interatomic electron transfer in previous theoretical studies.[7,31] For pNA, the generalized Amber force field (GAFF) parameters were employed.[32,33] The molecular structure of pNA was determined by RHF/6-31G(d) under the constraint with C_{2v} symmetry using Gaussian 09.[34] The point charge on each atom of pNA was determined by the restrained electrostatic potential (RESP) method with DFT-B3LYP/6-31G(d) and TD-DFT-B3LYP/6-31G(d) for the ground and first excited states, respectively. We used the same molecular structure for the excited state as that for the ground state. The number of grid points for the solute–solvent 3D-RISM calculations was 128^3 with a grid width of 0.25 Å for Na^+ and 0.5 Å for the other cases.

Details of the parameters are given in the supplementary material. All calculations were conducted using the RISM integrated calculator (RISMiCal) program package developed by us.[35]

IV. RESULTS AND DISCUSSION

A. Nonequilibrium free-energy profiles

Figure 2 shows the free-energy profiles, $\tilde{F}_{\mathrm{R}}(z)$ and $\tilde{F}_{\mathrm{P}}(z)$, of all three model systems. They are plotted as the difference from

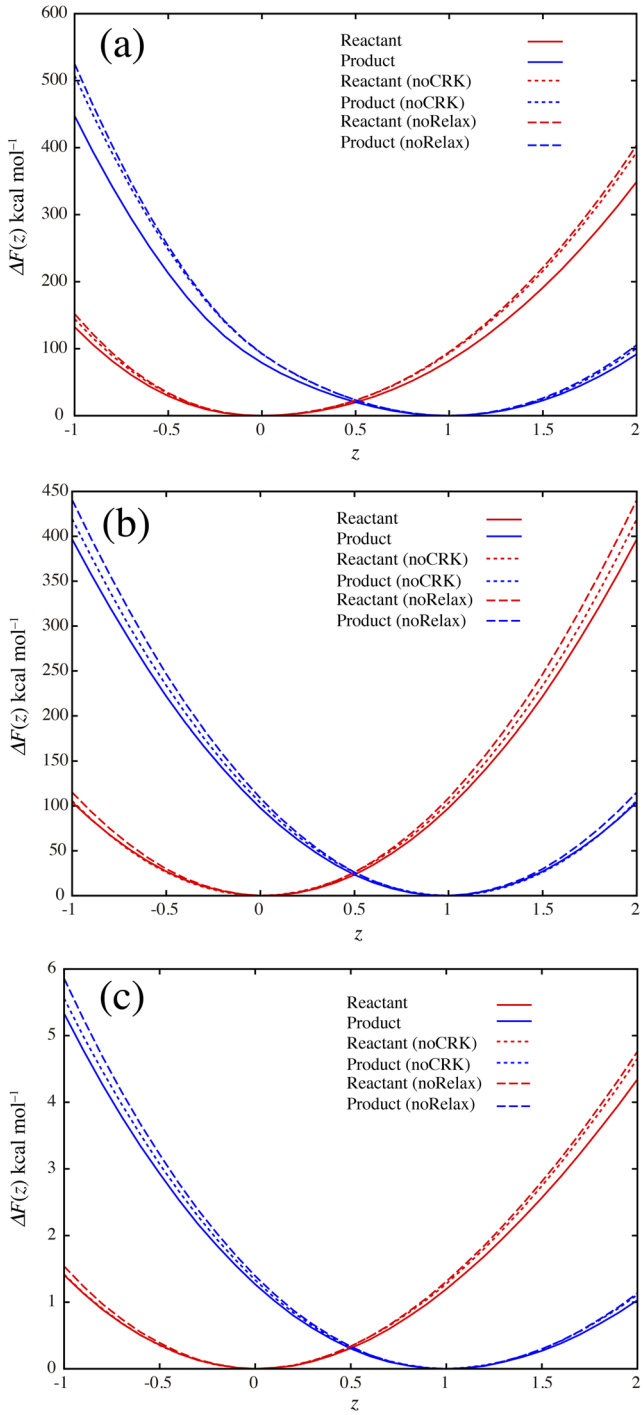

FIG. 2. Nonequilibrium free-energy profiles of three model systems plotted as a function of the coupling parameter z: (a) Na, (b) Fe–Fe, and (c) pNA. The left (red) and right (blue) parabolas correspond to the profiles for the reactant and product states, respectively, and are plotted as the difference from the equilibrium values, $F_R(0)$ and $F_P(1)$, for the reactant and product states, respectively. The results with and without (noCRK) the solvent electronic polarization are drawn with solid and dashed lines, respectively, and the profiles neglecting the relaxation of the electronic polarization (noRelax) are shown with dotted lines.

their respective equilibrium values, $\Delta\tilde{F}_R(z) \equiv \tilde{F}_R(z) - \tilde{F}_R(0)$ and $\Delta\tilde{F}_P(z) \equiv \tilde{F}_P(z) - \tilde{F}_P(1)$. All the profiles appear parabolic, and the curvatures of the reactant and product states seem to be close to each other, suggesting that the coupling between the charge transfer and the solvent reorganization is almost linear.

The free-energy profiles without inclusion of the electronic polarization of the solvent, referred to as "noCRK," are also shown in Fig. 2 for comparison. In this calculation, the point charges on the solvent sites are determined by solvent-polarizable DRISM (sp-DRISM) for the neat solvent. Therefore, the difference between this calculation and the full one indicates the effects of the deviation of the solvent polarization from the bulk one. In Fig. 2, we see that the inclusion of the solvent polarization reduces the curvature of the free-energy profile. In a linear system, the second derivative of $\tilde{F}_R(z)$ and $\tilde{F}_P(z)$ with respect to z is equal to 2λ, where λ means the solvent reorganization energy. Therefore, the decrease in the curvature means the decrease in the solvent reorganization energy, which is in agreement with previous studies based on molecular simulations, although the degree of the decrease is smaller in our theory than in previous simulations.[5,6,8]

Since the relaxation of the electronic polarization is as fast as the charge-transfer reaction, the electronic polarization maintains its equilibrium with the external electric field during slow fluctuation of the nuclear coordinate of the solvent. The relaxation reduces the nonequilibrium free energy. The amount of decrease of $\tilde{F}_R(z)$ is given by the last term of Eq. (28), $-\langle V_R(z;\Gamma)\rangle_z$. If the relaxation of the electronic polarization were as slow as the reorientational relaxation, the free-energy profile of the reactant state would be $\tilde{F}_R(z) + \langle V_R(z;\Gamma)\rangle_z$ instead of $\tilde{F}_R(z)$. The same also applies to the profile of the product state, $\tilde{F}_P(z)$. These hypothetical free-energy profiles, referred to as "noRelax," are also plotted in Fig. 2. As demonstrated in this figure, the relaxation of the electronic polarization actually decreases the free energy, as expected. The relative contribution of the polarization relaxation is a little larger for Na than for the other two (Fe–Fe and pNA). This quantitative aspect will be discussed in detail in Sec. IV D in relation to the dielectric continuum models.

The difference between $\tilde{F}_R(z)$ without electronic polarization and $\tilde{F}_R(z) + \langle V_R(z;\Gamma)\rangle_z$ with electronic polarization can be regarded as the effect of the local change in rigid charges on solvent sites around the solute. In all three systems, the latter is a little larger than the former, suggesting that the local change in the partial charge might destabilize the nonequilibrium state if the relaxation of the electronic polarization is absent. The destabilization is negligible in the Na case, while it is half as large as $V_R(z;\Gamma)_z$ in the other two cases. The difference will be analyzed from the viewpoint of the local solvation structure (Sec. IV C).

B. Solvation structure and local polarization

Before proceeding to the analysis of the nonequilibrium free-energy profiles, shown in Fig. 2, we first report on the solvation structures obtained by our sp-3D-RISM theory. Since the nuclear coordinates are frozen on charge transfer, the site distribution functions of the solvent, $g_O(\boldsymbol{r})$ and $g_H(\boldsymbol{r})$, are determined uniquely for a given value of z. On the other hand, the polarization charge densities, $g_O(\boldsymbol{r})\delta\Delta Q_O(\boldsymbol{r})$ and $g_H(\boldsymbol{r})\delta\Delta Q_H(\boldsymbol{r})$, depend on not only z but also the electronic state of the solute.

Figure 3 shows the solvation structure of the first model system, the Na atom in water. The solvation structure of the neutral reactant state, $z = 0$, is weakly structured, and both O and H atoms can contact with the Na atom, as exhibited by the peaks around 3 Å. With an increase in the charge on the solute (z), both the translational and orientational structures are strengthened. At $z = 1$, the large contact peak of $g_O(r)$ at 2.4 Å and the strong oscillation at the longer distance indicate a rigid and strong solvation structure. The first peak of $g_H(r)$ appears at a longer distance than that of $g_O(r)$, indicating that the H atom of the water molecule in the first solvation shell shows outward orientation because of the strong electric field of the solute.

The polarization charge densities are plotted in Fig. 4. At the equilibrium solvation structure, $z = 0$, electronic polarization is quite weak in the reactant state [see Fig. 4(a)] because the solute does not exert any electric field on the solvent. After the charge transfer, the solvent sites in contact with Na^+ exhibit strong negative polarization charges [Figs. 4(c) and 4(d)]. Since both the O and H atoms can orient toward the Na almost equally at $z = 0$, the heights of their negative peaks are also close to each other [Fig. 4(c)]. In the solvation structure at $z = 1$, the product state (Na^+) induces strongly negative polarization mainly on the O atom because the H atoms of water orient outward [Fig. 4(d)]. On the other hand, the polarization charge densities of both atoms are positive at $z = 1$ and in the reactant state [Fig. 4(b)]. The total charge density in the vicinity of the solute is negative in the solvation structure of Na^+ to screen the positive charge of the solute. In the reactant state of the solute, however, since the negative charge of the solvent is not canceled by the solute charge, positive electronic polarization is induced.

Figure 5 shows the site distribution functions around the Fe–Fe ion pair at $z = 0$ and $z = 0.5$. The results at $z = 1$ are omitted because of the symmetric nature of the reactant and product. Both ions are solvated by the O atom of water because of the positive charges on the ions. The solvation of Fe^{3+} is stronger than that of Fe^{2+} at $z = 0$, and the distribution becomes symmetric at $z = 0.5$.

Figure 6 demonstrates the polarization charge densities around the reactant at $z = 0$ and 1. Again, the results of the product state can be omitted because of the symmetry. At both of these values of z, the electronic polarization is stronger around Fe^{3+} than Fe^{2+}, ascribed, of course, to the stronger electric field of the former. Upon comparing $z = 0$ and 1, we note that the polarization around Fe^{3+} becomes stronger, whereas that around Fe^{2+} becomes weaker at $z = 1$. Since the screening around Fe^{3+} due to the orientational polarization becomes weaker at $z = 1$, the electric field on the electronic polarization must be stronger. The weaker polarization around Fe^{2+} can be explained in the same way.

The solvation structures of pNA in the reactant and product states are shown in Fig. 7. The change in the solvation structure on charge transfer is small compared with that in the former two systems (Na and Fe–Fe); this is explained by the relatively small change in the partial charges on the solute sites, as presented in Table S-I of the supplementary material. A notable difference is that small peaks of the H atom around the nitro group, representing the H bond between the O atom of the nitro group and the H atom of water, are weakened in the product state. The weakening is ascribed to the decrease in the amount of negative charge on the nitro oxygen presented in Fig. S1 of the supplementary material.

The polarization charge densities around pNA are plotted in Fig. 8. In the equilibrium states of the reactant and product, the change in the polarization charge density is similar to that in the site density distribution in Fig. 7. In the nonequilibrium state, $z = 1$ of the reactant, the negative polarization charge on the H atom around the nitro group increases from $z = 1$ of the product because of the increase in the negative charge on the nitro oxygen.

C. Solvent reorganization induced by electronic polarization

As briefly described in Sec. IV A, the change in the nonequilibrium free-energy profile upon the introduction of the electronic polarization into the solute–solvent system can be divided into two effects. The first is the effect of the local change in the partial charge on solvent sites, and the second is the effect of the relaxation of the electronic polarization after the charge

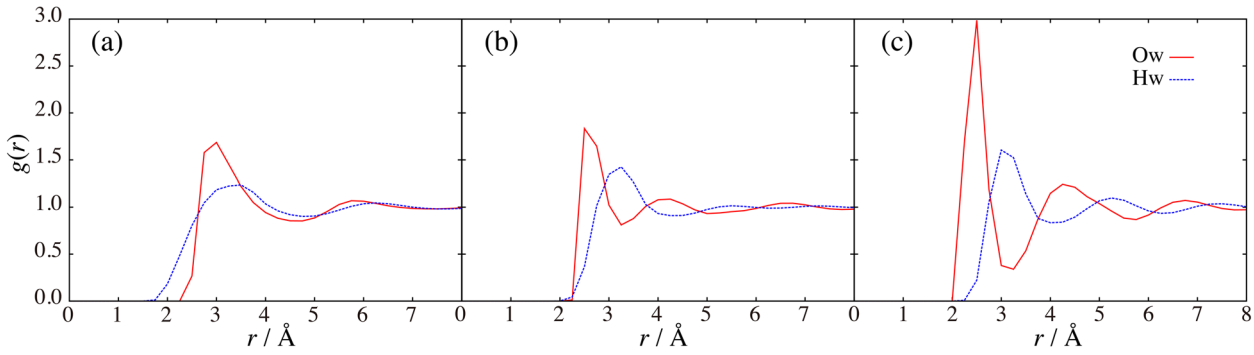

FIG. 3. Radial distribution functions around Na in water at (a) $z = 0$, (b) $z = 0.5$, and (c) $z = 1$. Red solid curves: distribution functions of the O atoms and blue dotted curves: distribution functions of the H atoms.

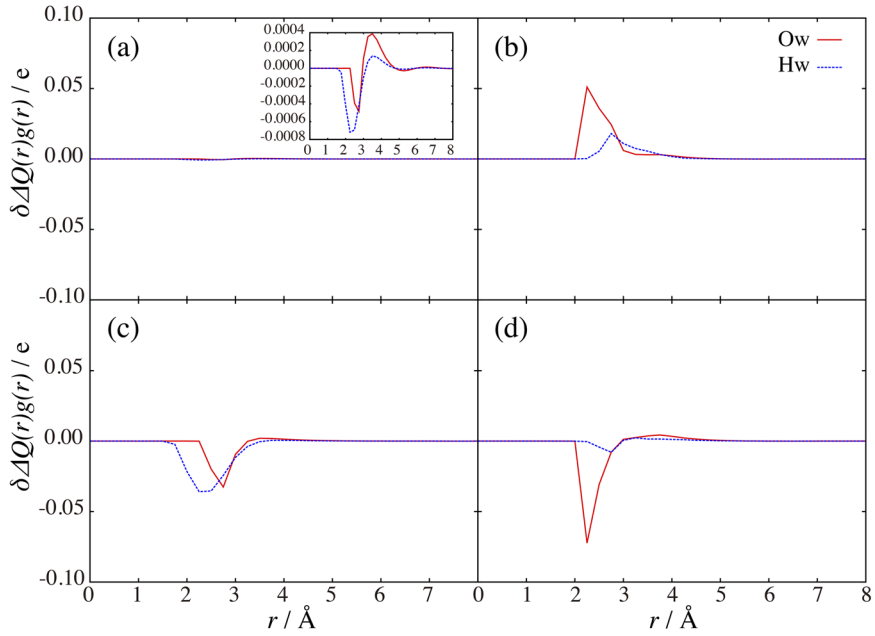

FIG. 4. Polarization charge densities, $g_O(\boldsymbol{r})\delta\Delta Q_O(\boldsymbol{r})$ and $g_H(\boldsymbol{r})\delta\Delta Q_H(\boldsymbol{r})$, around Na in water: (a) reactant at $z = 0$, (b) reactant at $z = 1$, (c) product at $z = 0$, and (d) product at $z = 1$. Inset shows the profiles in (a) enlarged. Red solid curves: polarization charges on the O atoms and blue dotted curves: polarization charges on the H atoms.

transfer. Their contributions, relative to the total free-energy difference, $\Delta\check{F}_R(z)$ or $\Delta\check{F}_P(z)$, were determined for all three model systems (see Table I).

In this subsection, we examine the first contribution of the local partial charges. In all three systems, this contributes to increasing the nonequilibrium free energy, and the contributions vary among the different systems. In Table I, the first Na system is hardly affected by the local change in the partial charge, whereas notable contributions are observed in the Fe–Fe and pNA systems. Within the same system, the magnitude of its relative contribution appears to increase with an increase in deviation from the equilibrium state.

In our sp-3D-RISM theory, the solute–solvent interaction is renormalized from $u_v(\boldsymbol{r})$ to $u_v^{\mathrm{CRK}}(\boldsymbol{r})$ by including the electronic polarization of the solvent. The solvent distribution around a solute is thereby rearranged, reflecting the renormalization. In Fig. 9, the degrees of the rearrangement are demonstrated for our three model systems.

In Fig. 9(a), the rearrangement of the solvation structure around the Na^+ ion is small. This is because the solvation shell of Na^+ is already structured and there is little room for the rearrangement. The rearrangement around a neutral Na atom is further negligible (results not shown here for the sake of brevity) because the electronic polarization within the solvation shell is small. On the other hand, a large rearrangement is observed around the Fe–Fe ion pair in Figs. 9(b) and 9(c). The largest magnitude of the difference in $g_O(\boldsymbol{r})$ amounts to unity. The rearrangement is particularly large around the Fe^{3+} ion because solvents are strongly polarized there. The distance between the Fe^{3+} ion and the O atom of water is shortened because of the increased attractive interaction between them. Although the rearrangement around pNA is not as large as that in the case of the Fe–Fe ion pair, a large rearrangement is shown in Fig. 9(e), particularly around the nitro group, reflecting the strengthening of the hydrogen bond between the nitro group and solvent water.

When we compare Fig. 9 and Table I, we note that the degree of the rearrangement correlates fairly well with the modification of the nonequilibrium free energy. In the Na system, the rearrangement is almost negligible [Fig. 9(a)], and the free energy is hardly affected by the local change in the partial charge. On the other hand, the modification of the free energy is not negligible in the Fe–Fe ion pair and pNA systems, where rearrangements of the solvation structures are notable.

In summary, the increase in the nonequilibrium free energy through the local change in the partial charges can be ascribed to the rearrangement of the solvation structure due to the renormalization of the solute–solvent interaction. Since the rearrangement stabilizes the equilibrium state, the nonequilibrium state is relatively destabilized, leading to an increase in the nonequilibrium free energy. The z-dependence of the relative contribution of the rearrangement, shown in the third column of Table I, can also be ascribed to the nonlinearity in the rearrangement.

D. Relaxation of electronic polarization: Comparison with dielectric continuum model

In this subsection, the effect of the relaxation of the electronic polarization after charge transfer of the solute is analyzed. Its relative contributions in the three model systems are summarized in the fourth column of Table I. Its value depends only slightly on both the value of z and the electronic state of the solute within the same system. When we compare the three systems, we see that the relative contributions in the Fe–Fe ion pair and pNA systems are close to each other and that the relaxation makes a larger contribution in the Na system.

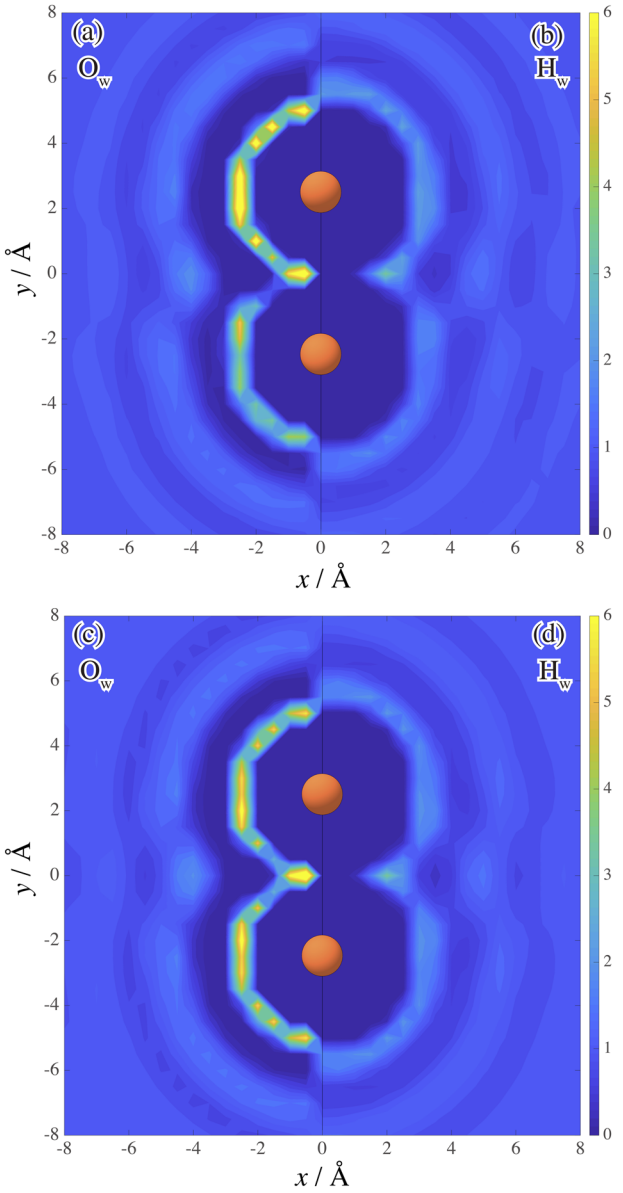

FIG. 5. Contour plots of the site distribution functions around the Fe–Fe ion pair: (a) $z = 0$, O atom, (b) $z = 0$, H atom, (c) $z = 0.5$, O atom, and (d) $z = 0.5$, H atom. The two red spheres at ± 2.5 Å indicate the positions of the two Fe ions. The upper and lower ions are Fe^{3+} and Fe^{2+}, respectively, in the reactant state.

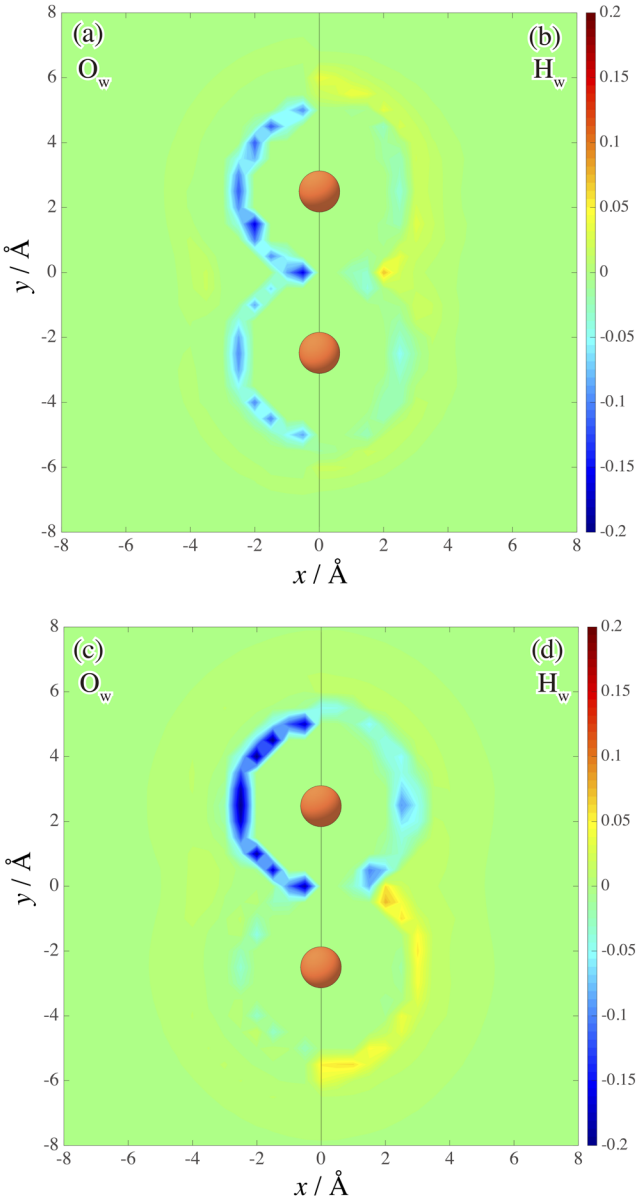

FIG. 6. Contour plots of the polarization charge densities around the reactant state of the Fe–Fe ion pair: (a) $z = 0$, O atom, (b) $z = 0$, H atom, (c) $z = 1$, O atom, and (d) $z = 1$, H atom.

The dielectric continuum model can be regarded as a first approximation for the nonequilibrium free-energy profile of the charge-transfer reaction. In the simplest dielectric continuum models, the solute is approximated as the cavity of radius a, possessing a point charge (monopole case) or a point dipole (dipole case) at the center of the cavity. The magnitude of the point charge or the point dipole changes upon the charge-transfer reaction, and the electric work to polarize the surrounding dielectric medium is determined.

The nonequilibrium free-energy profile of the reactant in the monopole case is given by

$$\tilde{F}_R(z) = \left[\frac{\epsilon - 1}{\epsilon} - \frac{\epsilon_\infty - 1}{\epsilon_\infty}\right]\frac{[Q(z) - Q(0)]^2}{2a}, \tag{40}$$

where ε and ε_∞ are the dielectric constants in the low- and high-frequency limits, respectively. The point charges in the reactant and

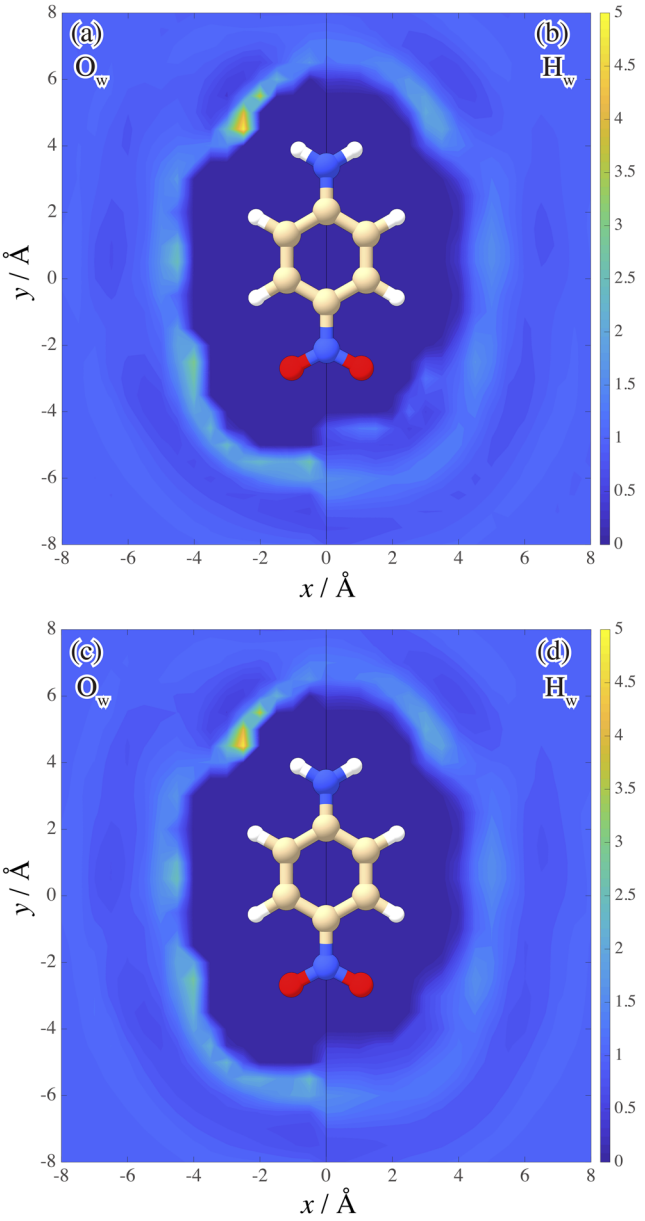

FIG. 7. In-plane contour plots of the site distribution functions around pNA: (a) $z = 0$, O atom, (b) $z = 0$, H atom, (c) $z = 1$, O atom, and (d) $z = 1$, H atom.

product states are denoted as $Q(0)$ and $Q(1)$, respectively, and that of the intermediate z-state is given by $Q(z) \equiv (1 - z)Q(0) + zQ(1)$. In the dipole case, the corresponding equation is

$$\tilde{F}_{\mathrm{R}}(z) = \left[\frac{\epsilon - 1}{2\epsilon + 1} - \frac{\epsilon_\infty - 1}{2\epsilon_\infty + 1}\right]\frac{|\boldsymbol{d}(z) - \boldsymbol{d}(0)|^2}{a^3}, \tag{41}$$

where $\boldsymbol{d}(0)$, $\boldsymbol{d}(1)$, and $\boldsymbol{d}(z) \equiv (1 - z)\boldsymbol{d}(0) + z\boldsymbol{d}(1)$ denote the dipole moments of the reactant, product, and z-states, respectively. The

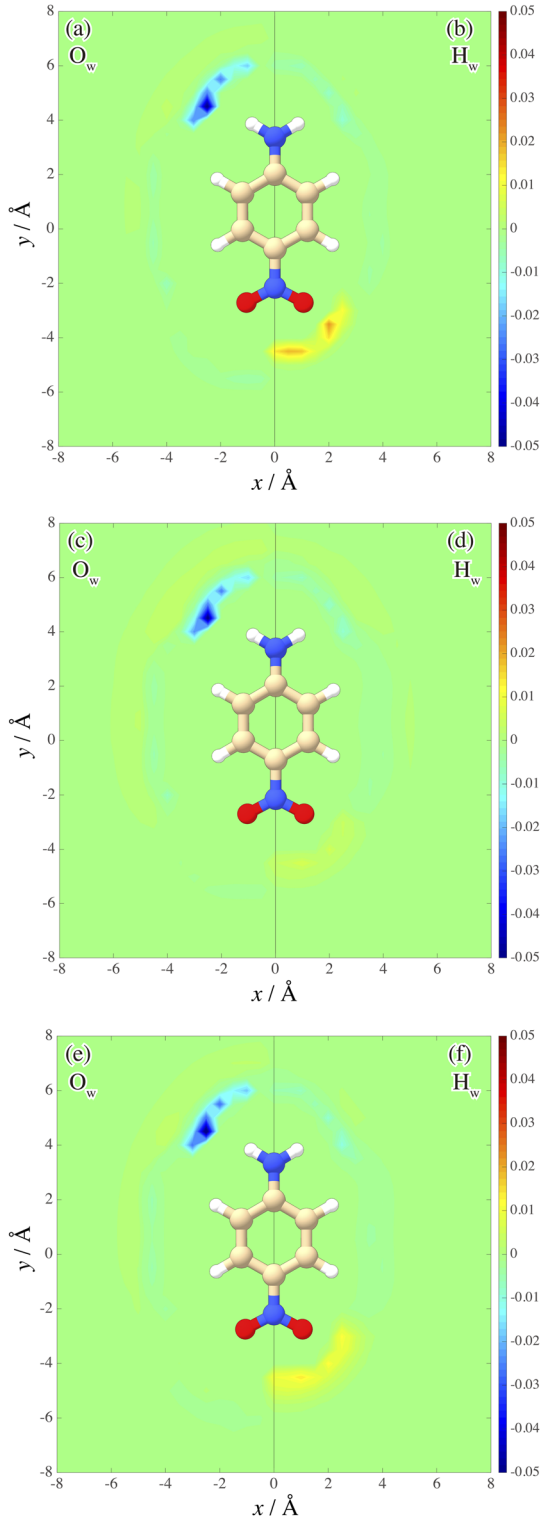

FIG. 8. In-plane contour plots of polarization charge densities around pNA: [(a) and (b)] the reactant state at $z = 0$, [(c) and (d)] the product state at $z = 1$, and [(e) and (f)] the reactant state at $z = 1$.

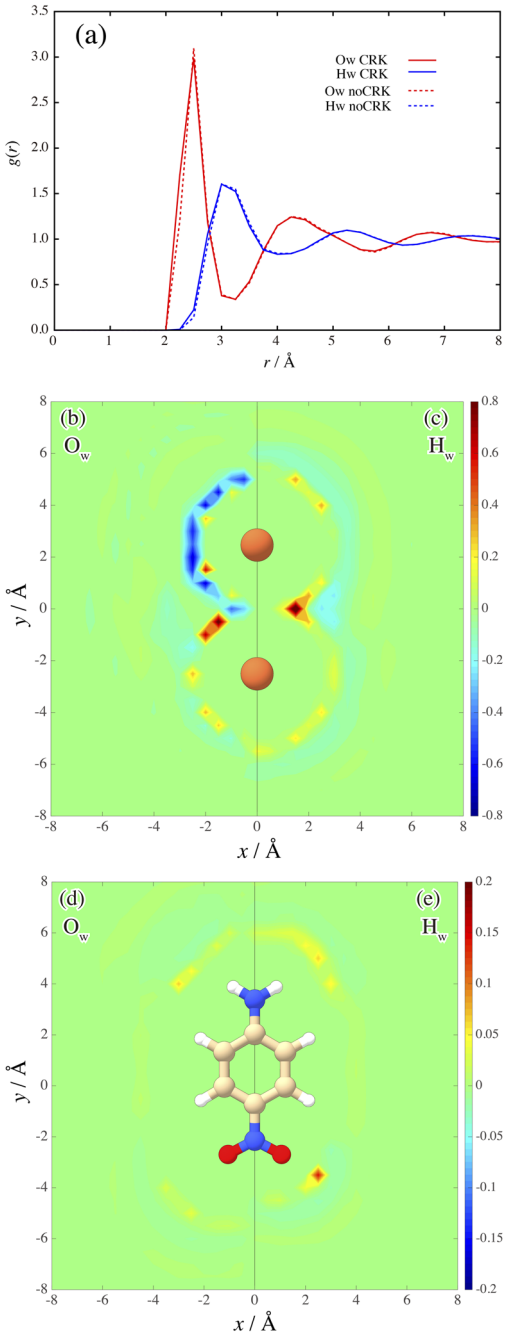

FIG. 9. Comparison between the solvation structures with and without including the electronic polarization of the solvent for the calculation of solute–solvent systems. In (a), the radial distribution functions around the Na^+ ion are plotted. The functions with and without the electronic polarization are shown with solid and dotted lines, respectively, and the red and blue lines indicate $g_O(r)$ and $g_H(r)$, respectively. In (b)–(e), the site distribution functions with the electronic polarization are subtracted from the corresponding functions without polarization and exhibited as the contour plots. Panels (b) and (c) show the results on the Fe–Fe ion pair in the reactant state. Panels (d) and (e) show the results on the pNA system in the reactant state. In these panels, $g_O(\boldsymbol{r})$s are shown in (b) and (d), and $g_H(\boldsymbol{r})$s are shown in (c) and (e).

derivation of Eqs. (40) and (41) is given in Sec. S-II of the supplementary material, and the profiles of the product state can be derived in the same way. In Eq. (41), the factor in the square bracket is equal to the polarity factor proposed by Mataga *et al.*[36] and Lippert[37] for the fluorescence Stokes shift.

As explained in the derivation in Sec. S-II of the supplementary material, the second factors in the square brackets in Eqs. (40) and (41) originate from the relaxation of the electronic polarization. Therefore, the relative contributions can be determined in terms of the ratio of the two terms in the square brackets without specifying the cavity size and dipole moment. Since the free-energy profiles are parabolic and their curvatures are independent of the electronic state of the solute in the dielectric continuum model, the relative contribution of the electronic relaxation is also independent of the value of z and the electronic state of the solute, which is in agreement with our sp-3D-RISM calculation.

The numerical values of the relative contributions are summarized in the last two lines of Table I. In the calculation, the reorientational part of the dielectric constant, $\epsilon_{np} \equiv \epsilon - \epsilon_\infty + 1$, is set to be the input value of DRISM, 78.5. The high-frequency dielectric constant, $\epsilon_\infty = 1.255$, is calculated from CRK using the theoretical formula of the sp-3D-RISM theory.[23] The values of the third column, the relative contribution of the reorganization of the solvation structure, are also calculated from the variation in the first factors in the square brackets of Eqs. (40) and (41), $1 - \frac{1}{\epsilon}$ and $\frac{\epsilon-1}{2\epsilon+1}$, with changing the low-frequency dielectric constant from ε to ε_{np}. Although their values are not exactly equal to zero, they are described as "0" because their absolute values are as small as 10^{-3}.

Our first model system, the Na atom in water, corresponds to the monopole case in the dielectric continuum model. The other two systems, the Fe–Fe ion pair and pNA, are close to the dipole case because the total charge on the solute is conserved on charge transfer. The theoretical value of the relative contribution of the relaxation of the electronic polarization is larger for the monopole than for the dipole case. This is in agreement with our sp-3D-RISM calculation, where the relaxation makes a larger relative contribution to the Na system than to the other two systems. On the other hand, the absolute values of the relative contribution are about 60%–70% of the prediction of the dielectric continuum model. Since our theory includes microscopic interaction and solvation structure that are neglected in the dielectric continuum model, we believe that the deviation could be ascribed to the latter.

The decrease in the reorganization energy, by including the electronic polarization, is about 10%, while about a 50% decrease has been reported in molecular simulation studies.[5,6,8] We consider that one of the reasons for this discrepancy is that the high-frequency dielectric constant, ε_∞, is underestimated in our theory. The theoretical value is 1.25, while the experimental one is 1.78. As we have discussed in our previous work, there are two reasons for the underestimation of ε_∞.[23] First, the out-of-plane electronic polarization is not described by CRK in the three-site model of water. Second, the theoretical relationship between CRK and ε_∞ predicts ε_∞ smaller than the classical Lorentz–Lorenz equation, probably because of the partial loss of the orientational correlation in the interaction-site model.

TABLE I. Relative contributions of the local change in the partial charges (third column) and the relaxation of the electronic polarization (fourth column). Their mathematical definitions are given in their captions. In the caption of the third column, "noCRK" means the calculation of free energy without including the electronic polarization for the solute–solvent system. In third and fourth columns, X stands for R (reactant) or P (product).

System	Condition	$\frac{\Delta\tilde{F}_X(z)+\langle V_X(z;\Gamma)\rangle_z-\Delta\tilde{F}_X(z;noCRK)}{\Delta\tilde{F}_X(z)}\times 100$ (%)	$\frac{\langle V_X(z;\Gamma)\rangle_z}{\Delta\tilde{F}_X(z)}\times 100$ (%)
Na	z = 0, X = P	0	17
	z = 0.5, X = P	0	16
	z = 0.5, X = R	−1	16
	z = 1, X = P	−2	16
Fe–Fe	z = 0, X = P	−5	11
	z = 0.5, X = P	−1	12
	z = 0.5, X = R	−1	12
	z = 1, X = P	−5	11
pNA	z = 0, X = P	−5	10
	z = 0.5, X = P	−3	10
	z = 0.5, X = R	0	10
	z = 1, X = P	−3	9
Continuum	Monopole[a]	0	26
	Dipole[b]	0	17

[a]Calculated by Eq. (40).
[b]Calculated by Eq. (41).

V. SUMMARY

A theoretical method is proposed to calculate the nonequilibrium free-energy profile of the charge-transfer reaction in solvents with electronic polarization based on the sp-3D-RISM theory that we have proposed in our previous work. The formula of the nonequilibrium free-energy profile was derived first in thermodynamic and statistical mechanical ways and then applied to three representative model systems.

Theoretical analysis suggests that the electronic polarization modifies the free-energy profile in two different ways. The first is the reorganization of the solvation structure through the renormalization of the solute–solvent interaction, and the second is the relaxation of the electronic polarization after the charge transfer. The first leads to the relative destabilization of the nonequilibrium state through the stabilization of the equilibrium state, and the second stabilizes the nonequilibrium state through the solvation of the nonequilibrium state by polarization charges. In our model systems, the second contribution is larger than the first, resulting in a decrease in the solvent reorganization energy, as has been reported in previous molecular simulation studies. The degree of the decrease in the reorganization energy is smaller than that in these simulation studies, which may be ascribed to the underestimation of the high-frequency dielectric constant.

SUPPLEMENTARY MATERIAL

See the supplementary material for the derivations and data that support the findings of this study, the derivations of the reciprocal relations [Eqs. (15) and (16)], the dielectric continuum models [Eqs. (40) and (41)], and force field parameters.

ACKNOWLEDGMENTS

We are grateful for the financial support from JSPS KAKENHI (Grant No. 19H02677). N.Y. acknowledges the Toyota Riken Scholar from the Toyota Physical and Chemical Research Institute. Numerical calculations were conducted, in part, at the Research Center for Computational Science, Institute for Molecular Science, National Institutes of Natural Sciences. Molecular graphics were depicted with UCSF Chimera, developed by the Resource for Biocomputing, Visualization, and Informatics at the University of California, San Francisco.[38]

DATA AVAILABILITY

The data that support the findings of this study are available from the corresponding author upon reasonable request.

REFERENCES

[1]H. B. Gray and J. R. Winkler, Q. Rev. Biophys. **36**(3), 341–372 (2003).
[2]R. A. Marcus and N. Sutin, Biochim. Biophys. Acta, Rev. Bioenerg. **811**(3), 265–322 (1985).
[3]D. W. Small, D. V. Matyushov, and G. A. Voth, J. Am. Chem. Soc. **125**(24), 7470–7478 (2003).
[4]H. Nakano and H. Sato, J. Chem. Phys. **146**(15), 154101 (2017).
[5]T. Ishida, J. Phys. Chem. B **109**(39), 18558–18564 (2005).
[6]E. Vladimirov, A. Ivanova, and N. Rösch, J. Chem. Phys. **129**(19), 194515 (2008).
[7]R. A. Kuharski, J. S. Bader, D. Chandler, M. Sprik, M. L. Klein, and R. W. Impey, J. Chem. Phys. **89**(5), 3248–3257 (1988).
[8]G. King and A. Warshel, J. Chem. Phys. **93**(12), 8682–8692 (1990).
[9]F. Hirata, *Molecular Theory of Solvation* (Kluwer, Dordrecht, 2003).

[10]S.-H. Chong, S. Miura, G. Basu, and F. Hirata, J. Phys. Chem. **99**(26), 10526–10529 (1995).
[11]S.-H. Chong and F. Hirata, Mol. Simul. **16**(1-3), 3–17 (1996).
[12]H. Sato and F. Hirata, J. Phys. Chem. A **106**(10), 2300–2304 (2002).
[13]N. Yoshida, T. Ishida, and F. Hirata, J. Phys. Chem. B **112**(2), 433–440 (2008).
[14]A. Kovalenko and F. Hirata, J. Chem. Phys. **110**(20), 10095–10112 (1999).
[15]A. Kovalenko and F. Hirata, Phys. Chem. Chem. Phys. **7**(8), 1785–1793 (2005).
[16]D. Beglov and B. Roux, J. Phys. Chem. B **101**(39), 7821–7826 (1997).
[17]Q. Du, D. Beglov, and B. Roux, J. Phys. Chem. B **104**(4), 796–805 (2000).
[18]N. Yoshida, J. Chem. Inf. Model. **57**(11), 2646–2656 (2017).
[19]N. Yoshida, T. Imai, S. Phongphanphanee, A. Kovalenko, and F. Hirata, J. Phys. Chem. B **113**(4), 873–886 (2009).
[20]A. Morita and S. Kato, J. Am. Chem. Soc. **119**(17), 4021–4032 (1997).
[21]A. Morita and S. Kato, J. Chem. Phys. **108**(16), 6809–6818 (1998).
[22]K. Naka, A. Morita, and S. Kato, J. Chem. Phys. **111**(2), 481–491 (1999).
[23]N. Yoshida and T. Yamaguchi, J. Chem. Phys. **152**(11), 114108 (2020).
[24]R. A. Marcus, Discuss. Faraday Soc. **29**, 21–31 (1960).
[25]S. J. Singer and D. Chandler, Mol. Phys. **55**(3), 621–625 (1985).
[26]M. R. Reddy and M. Berkowitz, Chem. Phys. Lett. **155**(2), 173–176 (1989).
[27]S. Ten-no, F. Hirata, and S. Kato, J. Chem. Phys. **100**(10), 7443–7453 (1994).
[28]J. S. Perkyns and B. M. Pettitt, Chem. Phys. Lett. **190**(6), 626–630 (1992).
[29]J. Aqvist, J. Phys. Chem. **94**(21), 8021–8024 (1990).
[30]P. Wolohan, J. Yoo, M. J. Welch, and D. E. Reichert, J. Med. Chem. **48**(17), 5561–5569 (2005).
[31]B. L. Tembe, H. L. Friedman, and M. D. Newton, J. Chem. Phys. **76**(3), 1490–1507 (1982).
[32]J. Wang, R. M. Wolf, J. W. Caldwell, P. A. Kollman, and D. A. Case, J. Comput. Chem. **25**(9), 1157–1174 (2004).
[33]J. Wang, W. Wang, P. A. Kollman, and D. A. Case, J. Mol. Graphics Modell. **25**(2), 247–260 (2006).
[34]G. W. T. M. J. Frisch, H. B. Schlegel, G. E. Scuseria, M. A. Robb, J. R. Cheeseman, G. Scalmani, V. Barone, G. A. Petersson, H. Nakatsuji, X. Li, M. Caricato, A. Marenich, J. Bloino, B. G. Janesko, R. Gomperts, B. Mennucci, H. P. Hratchian, J. V. Ortiz, A. F. Izmaylov, J. L. Sonnenberg, D. Williams-Young, F. Ding, F. Lipparini, F. Egidi, J. Goings, B. Peng, A. Petrone, T. Henderson, D. Ranasinghe, V. G. Zakrzewski, J. Gao, N. Rega, G. Zheng, W. Liang, M. Hada, M. Ehara, K. Toyota, R. Fukuda, J. Hasegawa, M. Ishida, T. Nakajima, Y. Honda, O. Kitao, H. Nakai, T. Vreven, K. Throssell, J. A. Montgomery, Jr., J. E. Peralta, F. Ogliaro, M. Bearpark, J. J. Heyd, E. Brothers, K. N. Kudin, V. N. Staroverov, T. Keith, R. Kobayashi, J. Normand, K. Raghavachari, A. Rendell, J. C. Burant, S. S. Iyengar, J. Tomasi, M. Cossi, J. M. Millam, M. Klene, C. Adamo, R. Cammi, J. W. Ochterski, R. L. Martin, K. Morokuma, O. Farkas, J. B. Foresman, and D. J. Fox, Gaussian 09, Revision A.02 (Gaussian, Inc., 2016).
[35]N. Yoshida, IOP Conf. Ser.: Mater. Sci. Eng. **773**, 012062 (2020).
[36]N. Mataga, Y. Kaifu, and M. Koizumi, Bull. Chem. Soc. Jpn. **28**(9), 690–691 (1955).
[37]E. Lippert, Z. Naturforsch. A **10**(7), 541–545 (1955).
[38]E. F. Pettersen, T. D. Goddard, C. C. Huang, G. S. Couch, D. M. Greenblatt, E. C. Meng, and T. E. Ferrin, J. Comput. Chem. **25**(13), 1605–1612 (2004).